



# A study of highly conductive ester co-solvents in Li[Ni<sub>0.5</sub>Mn<sub>0.3</sub>Co<sub>0.2</sub>]O<sub>2</sub>/Graphite pouch cells

Xiaowei Ma <sup>a</sup>, Jing Li <sup>a</sup>, Stephen L. Glazier <sup>a</sup>, Lin Ma <sup>b</sup>, Kevin L. Gering <sup>c</sup>, J.R. Dahn <sup>a, b, \*</sup>

<sup>a</sup> Department of Physics and Atmospheric Science, Dalhousie University, Halifax, Nova Scotia, B3H 3J5, Canada

<sup>b</sup> Department of Chemistry, Dalhousie University, Halifax, Nova Scotia, B3H 4R2, Canada

<sup>c</sup> Department of Biological & Chemical Processing, Idaho National Laboratory, 2525 Fremont Ave., Idaho Falls, ID 83415-3732, USA

## ARTICLE INFO

### Article history:

Received 20 January 2018

Received in revised form

1 March 2018

Accepted 1 March 2018

Available online 2 March 2018

### Keywords:

Rapid charge

Ester co-solvents

Electrolyte conductivity

Electrolyte viscosity

Long lifetime lithium-ion cells

## ABSTRACT

The effect of low viscosity esters on rate capability and lifetime of Li[Ni<sub>0.5</sub>Mn<sub>0.3</sub>Co<sub>0.2</sub>]O<sub>2</sub>/graphite pouch cells was studied using a variety of methods including ultra high precision coulometry, isothermal calorimetry and long term cycle testing. Methyl acetate (MA) and methyl propionate (MP) were selected as the ester co-solvents in ethylene carbonate (EC): ethyl methyl carbonate (EMC): dimethyl carbonate (DMC) (25:5:70 vol%) blended solvent along with 2% vinylene carbonate (VC) or 2% fluoroethylene carbonate (FEC) additives. Cells containing electrolytes with 20% or 40% MA or MP could support higher charging rates without unwanted lithium plating than those without esters. All electrolytes with 2% FEC could support higher charging rates without unwanted lithium plating compared to corresponding electrolytes with 2% VC. However, UHPC and microcalorimetry measurements indicate that both the use of esters and the use of FEC over VC lead to lifetime penalties which were confirmed by long term cycling tests. Useful electrolytes, detailed in this report, that yield a good compromise between high charging rates and long lifetime are those that contain 20% MA by weight.

© 2018 Elsevier Ltd. All rights reserved.

## 1. Introduction

Rapid charging capability is desirable for electric vehicles equipped with Li-ion batteries (LIBs). Unfortunately, fast charging or low temperature charging can cause unwanted lithium plating on the graphite negative electrode of Li-ion cells, which can drastically reduce the capacity and cycle life of lithium ion cells [1–3]. Electrolytes with high conductivity and low viscosity can help enhance the charging rate capability of LIBs.

Esters with low freezing points and low viscosity can yield electrolytes with high ionic conductivity when used as co-solvents. Esters have been used in low temperature Li-ion cells to improve their performance, and the most interesting include methyl acetate (MA), methyl propionate (MP), ethyl acetate (EA), methyl butyrate (MB), ethyl butyrate (EB), ethyl propionate (EP), etc [4–12]. Unfortunately the improved low temperature performance is normally accompanied by degraded capacity retention during long-term cycling because esters with low molecular weight (e.g. EA)

are thought to react slowly with negative electrodes [4,5]. EA, MP and MB used as a sole electrolyte solvent along with appropriate electrolyte additives or as a co-solvent have been studied in Li [Ni<sub>0.33</sub>Mn<sub>0.33</sub>Co<sub>0.33</sub>]O<sub>2</sub>/graphite, Li[Ni<sub>0.42</sub>Mn<sub>0.42</sub>Co<sub>0.16</sub>]O<sub>2</sub>/graphite, LiCoO<sub>2</sub>/graphite and Li[Ni<sub>1-x-y</sub>Co<sub>x</sub>Al<sub>y</sub>]O<sub>2</sub>/Graphite-SiO pouch cells [13–15]. In this work, the effect of two typical esters, MA and MP, on rate capability as well as lifetime of Li[Ni<sub>0.5</sub>Mn<sub>0.3</sub>Co<sub>0.2</sub>]O<sub>2</sub>/graphite pouch cells were studied.

Ethyl methyl carbonate (EMC) and dimethyl carbonate (DMC) are two common linear carbonate co-solvents used in commercial lithium ion cells. Considering the different melting points and viscosities of DMC (4 °C and 0.59 cP at 20 °C) and EMC (–53 °C and 0.65 cP at 20 °C), their effects on the rate capability of Li [Ni<sub>0.5</sub>Mn<sub>0.3</sub>Co<sub>0.2</sub>]O<sub>2</sub>/graphite pouch cells were also investigated in this work.

## 2. Experimental section

### 2.1. Preparation and formation of pouch cells

All the chemicals were used as received from BASF: LiPF<sub>6</sub> (99.94% purity, water content 14 ppm), ethylene carbonate (EC):

\* Corresponding author. Department of Physics and Atmospheric Science, Dalhousie University, Halifax, Nova Scotia, B3H 3J5, Canada.

E-mail address: [jeff.dahn@dal.ca](mailto:jeff.dahn@dal.ca) (J.R. Dahn).

ethyl methyl carbonate (EMC) (30:70 wt%, water content 12.1 ppm), ethylene carbonate (EC): ethyl methyl carbonate (EMC): dimethyl carbonate (DMC) (25:5:70 vol%, water content 19.7 ppm), vinylene carbonate (VC), fluoroethylene carbonate (FEC), methyl acetate (MA, 99.9% purity, water content 5.2 ppm) methyl propionate (MP, 99.9% purity, water content 19.9 ppm).

Dry and sealed single crystal  $\text{Li}[\text{Ni}_{0.5}\text{Mn}_{0.3}\text{Co}_{0.2}]\text{O}_2/\text{graphite}$  pouch cells (230 mAh at 4.3 V) that were balanced for 4.5 V operation and do not contain electrolyte were obtained from Li-FUN Technology (Xinma Industry Zone, Golden Dragon Road, Tianyuan District, Zhuzhou City, Hunan Province, China, 412000). The single side coating active material electrode loadings were  $21.1 \text{ mg/cm}^2$  for the positive electrode and  $12.4 \text{ mg/cm}^2$  for the graphite negative electrode. The positive electrode consisted of 94 wt % active material and the negative electrode had 95.4 wt % active material. The positive electrode was compressed to a density of  $3.5 \text{ g/cm}^3$  and negative electrode was compressed to  $1.55 \text{ g/cm}^3$ . Prior to filing with the desired electrolyte, pouch cells were cut open and dried at  $100^\circ\text{C}$  under vacuum for 14 h to remove any residual moisture. Afterwards, pouch cells were filled with 0.85 mL electrolyte in an Ar-filled glove box and sealed with a pouch sealer (MSK-115 A Vacuum Sealing Machine) under vacuum at a pressure of  $-90 \text{ kPa}$  (relative to atmospheric pressure). Six electrolyte blends studied in this work included 1.2 M  $\text{LiPF}_6$  in EC:EMC, EC:EMC:DMC, 80 wt% EC:EMC:DMC +20 wt% MA, 60 wt% EC:EMC:DMC +40 wt% MA, 80 wt% EC:EMC:DMC +20 wt% MP, and 60 wt% EC:EMC:DMC +40 wt% MP. For each electrolyte blend, either 2 wt% VC or 2 wt% FEC were used as additives.

After filling, cells were held at 1.5 V for 24 h to promote wetting and subsequently moved to a  $40^\circ\text{C}$  box connected to a Maccor 4000 series charger. Pouch cells were charged to 4.3 V at a current corresponding to C/20, held at 4.3 V for 1 h and then discharged to 3.8 V at C/20. In order to remove the gas formed during the charging and discharging process, the pouch cells were cut open and resealed under vacuum in the glove box. Cells were moved for electrochemical impedance spectroscopy measurements.

## 2.2. Electrochemical impedance spectroscopy (EIS)

The electrochemical impedance spectra of the pouch cells were collected after formation, using a BioLogic VMP3 equipped with 2 EIS boards. All the measurements were performed at  $10.0 \pm 0.1^\circ\text{C}$  from 100. kHz to 10. mHz (10. mV input). A temperature of  $10^\circ\text{C}$  was selected to amplify the differences between cells with different ester and additive content.

## 2.3. Gas volume measurement

The gas production in pouch cells during formation and cycling was measured using Archimedes' principle. Each cell was suspended underneath a Shimadzu analytical balance (AUW200D) and weighed while submerged in nano-purified deionized (DI) water ( $18 \text{ M}\Omega\cdot\text{cm}$ ). The produced gas ( $\Delta v$ ) in each cell is proportional to the change in apparent cell weight ( $\Delta m$ ) that was caused by the buoyant force, as Equation (1):

$$\Delta V = -\Delta m/\rho \quad (1)$$

where  $\rho$  is the density of DI water.

## 2.4. High rate cycling, long-term cycling and the ultra high precision coulometry (UHPC) cycling

High rate cycling was performed at  $20. \pm 1^\circ\text{C}$ . The cells were charged and discharged between 3.0 and 4.3 V and the voltage was

held at 4.3 V at the top of charge until the current dropped below C/20. Each cell was first charged and discharged at C/5 ( $C = 210 \text{ mA}$ ) for 3 cycles. Subsequently, cells were cycled with sequentially increasing charge rates of 1C, 1.5C, 2C, 2.5C and 3C, respectively. The discharging rate was constantly set at C/3.30 cycles at each charging rate were applied. Cycling ended as unwanted lithium plating occurred. After each period of the high charge rate cycles, cells were charged and discharged at C/5 three times to determine the capacity retention and the existence of unwanted lithium plating using the methods in Ref. [2].

Long term cycling was performed at  $40.0 \pm 0.1^\circ\text{C}$  with an upper cut off potential of 4.3 V on a Neware testing system (Shenzhen, China). The cells were charged and discharged with a current corresponding to C/3 between 3.0 and 4.3 V and the voltage was held at 4.3 V at the top of charge until the current dropped below C/20.

The UHPC cycling was performed at  $40.0 \pm 0.1^\circ\text{C}$  using the UHPC charger at Dalhousie University and detailed descriptions of the method can be found in Ref. [16]. Cells were charged and discharged with a current corresponding to C/20 between 3.0 and 4.3 V.

## 2.5. Conductivity measurement

Electrolytic conductivity was measured using a Mettler Toledo FG3 conductivity meter. Before the measurement, the conductivity probe was calibrated using a conductivity standard (RICCA,  $12.88 \text{ mS/cm}$  at  $25^\circ\text{C}$ ). 10 mL of electrolyte was added to a Teflon holder under a fume hood. The probe was then sealed to the holder by an O-ring. The sealed Teflon holder with the electrolyte and conductivity probe was then placed in a temperature controlled bath (VWR Scientific model 1151) filled with a water/ethylene glycol mixture. Conductivity was measured at  $-20^\circ\text{C}$ ,  $0^\circ\text{C}$ ,  $20^\circ\text{C}$ ,  $40^\circ\text{C}$  and  $60^\circ\text{C}$ . At each temperature step, a constant temperature was maintained for at least 1 h to allow for the electrolyte temperature to equilibrate with the bath. Data was only considered valid after the temperature of the electrolyte was stable.

## 2.6. Isothermal microcalorimetry

The average parasitic heat flow of cells containing different amounts of EMC, DMC and MA co-solvents was measured using a TAM III Microcalorimeter at  $40. \pm 0.0001^\circ\text{C}$  (TA Instruments: stability  $\pm 0.0001^\circ\text{C}$ , accuracy  $\pm 1 \mu\text{W}$ , precision  $\pm 1 \text{ nW}$ ). The baseline drift over the course of the experiments did not exceed  $\pm 0.5 \mu\text{W}$ . All information regarding microcalorimetry calibration, cell connections, and operation procedures can be found in previous literature [17,18]. After formation, cells were connected to a Maccor 4000 series charger to be charged and discharged between 4.0 V and different upper cut-off potentials: 4.2 V, 4.3 V (twice) and again 4.2 V (twice) at 1 mA investigate the parasitic heat flow occurring in different voltage ranges.

## 2.7. Open-circuit voltage (OCV) storage

After formation, cells containing 0% MA or 20% MA in EC:EMC were discharged to 3 V and charged to 3.5, 4.0, 4.2 or 4.4 V two times with a current corresponding to C/10. Cells were then held at 3.5, 4.0, 4.2 or 4.4 V, respectively, for 24 h and afterwards transferred to storage boxes at 30, 40, or  $50.^\circ\text{C}$ , respectively. The open-circuit voltage was recorded automatically every 6 h for 500 h.

## 3. Results and discussion

Fig. 1a and b shows the calculated conductivity and viscosity versus the molality of  $\text{LiPF}_6$  in solvents with different EC:EMC:DMC

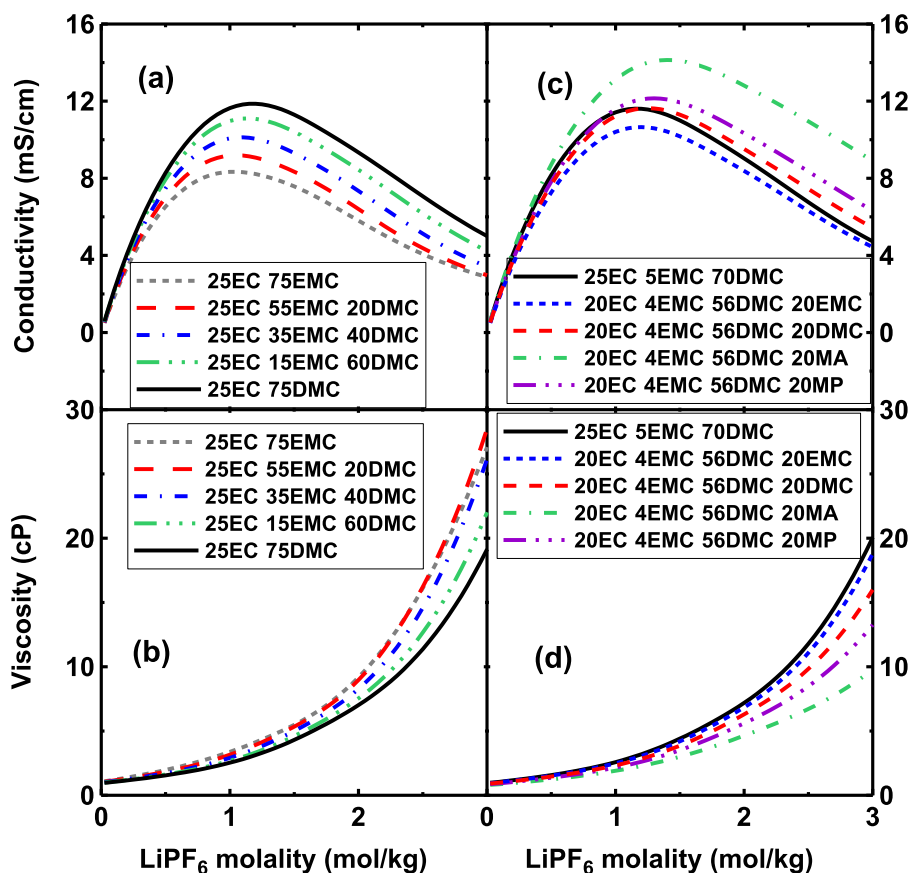


**Fig. 1.** (a) Calculated (Using AEM version 2.17.4 B) ionic conductivity of  $\text{LiPF}_6$  in EC:EMC:DMC electrolytes with different EMC:DMC ratios; (b) Calculated viscosity of  $\text{LiPF}_6$  in EC:EMC:DMC electrolytes with different EMC:DMC ratios; (c) Calculated ionic conductivity of  $\text{LiPF}_6$  in EC:EMC:DMC mixed with 20%EMC, 20%DMC, 20% MA or 20% MP; (d) Calculated viscosity of  $\text{LiPF}_6$  in EC:EMC:DMC mixed with 20% MA or 20% MP. All the calculations were performed at 20 °C.

ratios at 20 °C, using Gering's "Advanced Electrolyte Model", version 2.17.4 B [19–21]. Fig. 1a and b shows that the conductivity and viscosity of the EC:EMC:DMC ternary solvent blend are strongly influenced by the proportion of DMC. Larger amounts of DMC in the ternary blend yield higher conductivity and lower viscosity. Fig. 1c and d shows the calculated conductivity and viscosity versus the molality of  $\text{LiPF}_6$  in mixtures of EC:EMC:DMC (25:5:70) containing 20% MA or 20% MP. The results for EC:EMC:DMC (25:5:70) mixed with 20% EMC or 20% DMC (i.e. EC:EMC:DMC (20:24:56) or EC:EMC:DMC (20:4:76)) are also shown for comparison, and three EC:EMC:DMC blends follow the similar trends as in Fig. 1a and b. In comparison, the presence of ester co-solvents can further enhance the conductivity and decrease the viscosity of EC:EMC:DMC above 0.5 m  $\text{LiPF}_6$  for MA and above 1.0 m for MP. Comparing MA- and MP-containing EC:EMC:DMC solvents, MA is more beneficial than MP to improve the ionic conductivity.

Fig. 2 shows the calculated and measured conductivities of 1.2 M  $\text{LiPF}_6$  in EC:EMC:DMC:MA as a function of temperature between  $-20$  °C to 60 °C. The calculated conductivities agree well with the experimental values over the whole temperature range, except for a deviation for EC:EMC:DMC at  $-20$  °C. The ternary electrolyte blend is partially frozen at  $-20$  °C because DMC has a high freezing point at  $-4$  °C and the AEM does not take this freezing into account. Fig. 2 shows that the conductivity increases almost linearly with temperature for each electrolyte blend. At each temperature, the ionic conductivity increased significantly with increasing concentrations of MA.

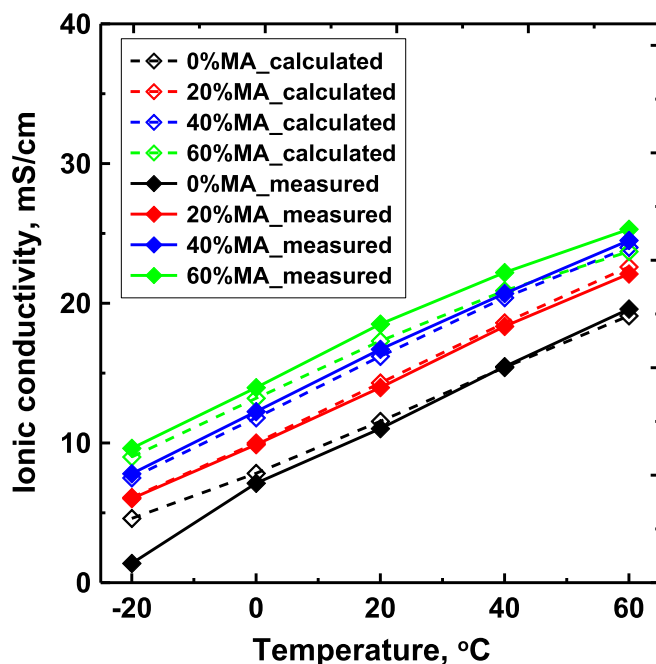


**Fig. 2.** Calculated (using AEM version 2.17.4 B) and measured ionic conductivity of 1.2 M  $\text{LiPF}_6$  in EC:EMC:DMC:MA between  $-20$  and 60 °C.

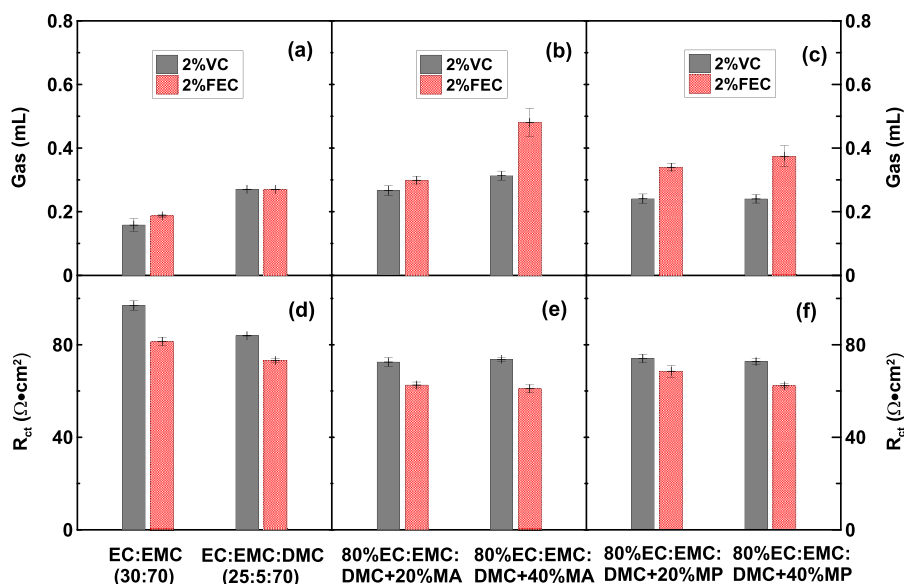


**Fig. 3.** Gas evolution (a to c) during formation ( $C/20$  at  $40^\circ\text{C}$ ) and  $R_{ct}$  after formation (measured at  $10^\circ\text{C}$ ) (d to f) of NMC532/AG pouch cells containing EC:EMC, EC:EMC:DMC, EC:EMC:DMC:MA and EC:EMC:DMC:MP solvents.

Fig. 3a, b and c shows the amount of gas produced during the formation of cells containing EC:EMC, EC:EMC:DMC and EC:EMC:DMC:ester blends with 2% VC or 2% FEC as additives. Fig. 3a shows that EC:EMC:DMC produced more gas than EC:EMC. Fig. 3b and c shows that 20% MA or 20% and 40% MP co-solvents did not increase gas production obviously compared to EC:EMC:DMC + 2% VC. 20% and 40% MP or 40% MA as co-solvents led to much larger amounts of gas than EC:EMC:DMC + 2% FEC. For each EC:EMC:DMC:ester solvent blend, 2%FEC as the additive induced more gas than when 2% VC was used as the additive. Fig. 3d, e and f shows  $R_{ct}$  of these cells measured as the diameter of the “semi-circle” in the Nyquist plot. Fig. 3d shows that the cells with EC:EMC:DMC have smaller  $R_{ct}$  values than cells with EC:EMC. Fig. 3e and f shows that adding esters further lowered  $R_{ct}$  of cells. In

contrast to gas formation, cells containing 2% FEC had smaller  $R_{ct}$  than cells containing 2% VC.

Fig. 4 shows the capacity versus cycle number of cells containing EC:EMC, EC:EMC:DMC and EC:EMC:DMC:ester solvents at  $20^\circ\text{C}$  with charge rates up to 3C. The cells were always discharged at  $C/2$ . These experiments were modelled after those developed by Liu et al. [2] In Fig. 4a, cells containing EC:EMC:DMC + 2% VC or EC:EMC:DMC + 2% FEC show better capacity retention than cells with EC:EMC + 2% VC or EC:EMC + 2% FEC, mainly due to the higher conductivity of DMC-containing electrolytes than EMC-containing electrolytes (see Fig. 1). Fig. 4a also shows that 2% FEC performed better than 2% VC as observed by the better capacity retention of cells using the same electrolyte solvent blend. However, none of cells exhibited ideal capacity retention at 2C due to unwanted

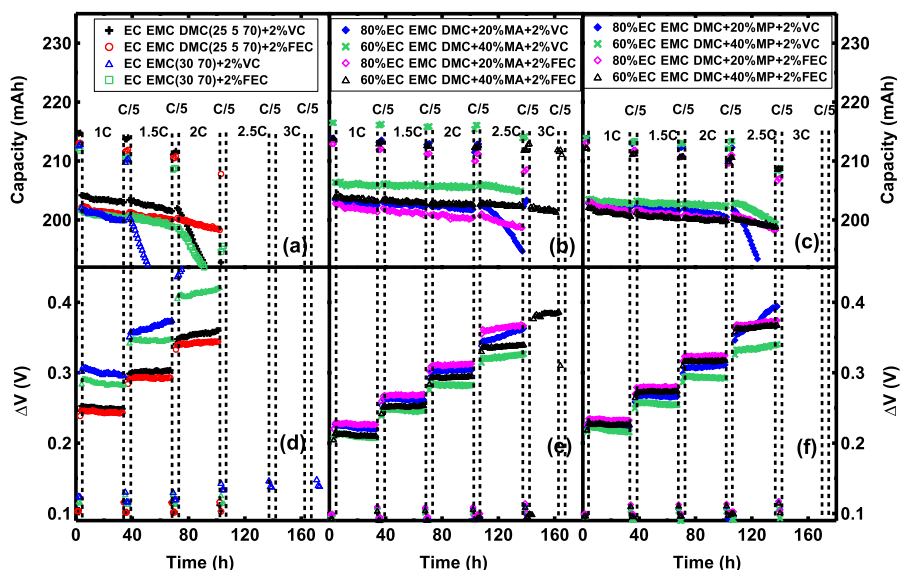


**Fig. 4.** Capacity versus cycle number (a to c) and  $\Delta V$  (d to f) of NMC532/graphite pouch cells containing MA and MP with charge rates from  $C/5$  to 3C at  $20^\circ\text{C}$ . The discharge was at  $C/2$  for all cycles.

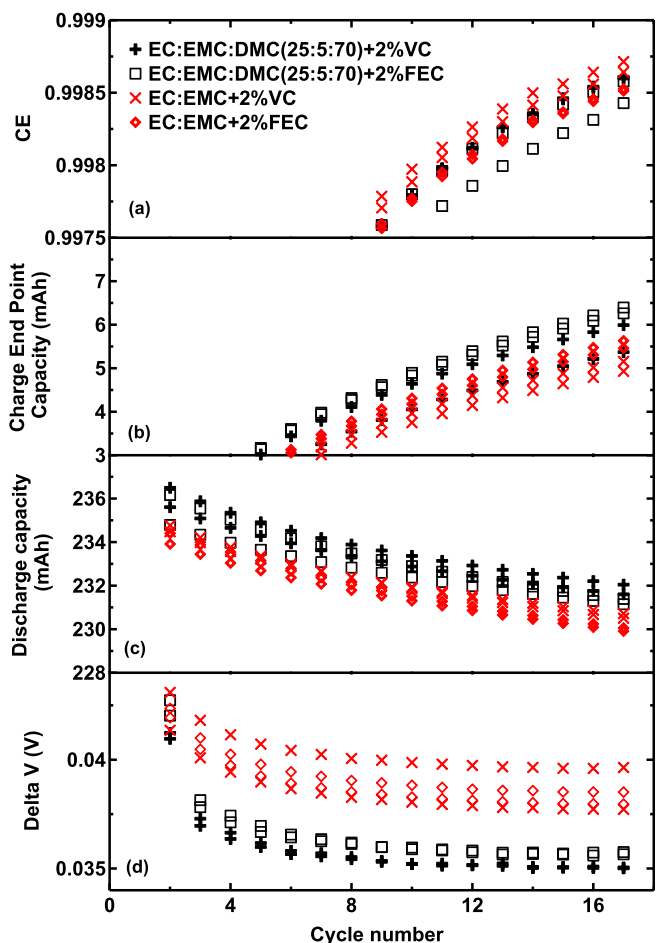


Fig. 5. Summary of UHPC data for NMC532/graphite pouch cells containing EC:EMC and EC:EMC:DMC solvents (3.0–4.3 V, C/20 and 40 ± 0.1 °C). (a) coulombic efficiency; (b) charge end point capacity; (c) discharge capacity; (d) ΔV.

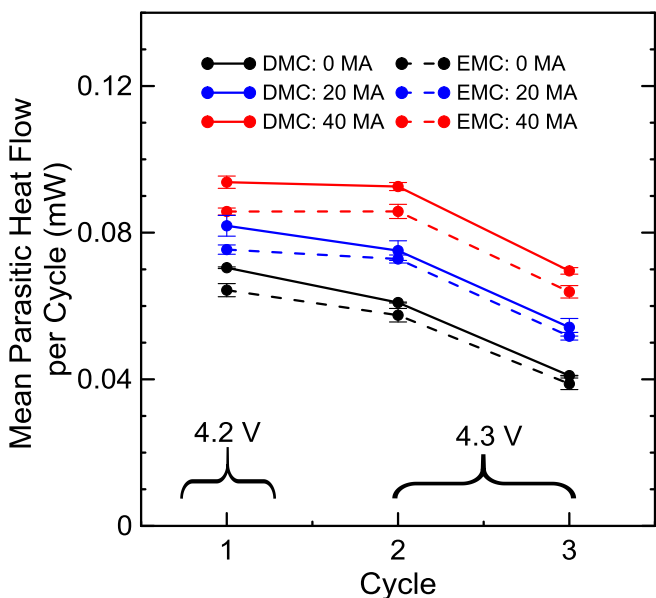


Fig. 6. Average parasitic heat flow of NMC532/graphite pouch cells containing different amounts of EMC, DMC or MA co-solvents and 2%FEC with upper cut off potential at 4.2 V and 4.3 V. The cells were cycled in narrow ranges at C/230 (1 mA) between 4.0 V and the indicated upper cutoff potential at 40 °C. When the legend indicates “DMC” it means the base solvent blend was EC:EMC:DMC 25:5:70 by volume. When the legend indicates “EMC” it means the base solvent blend was EC:EMC: 30:70 by weight.

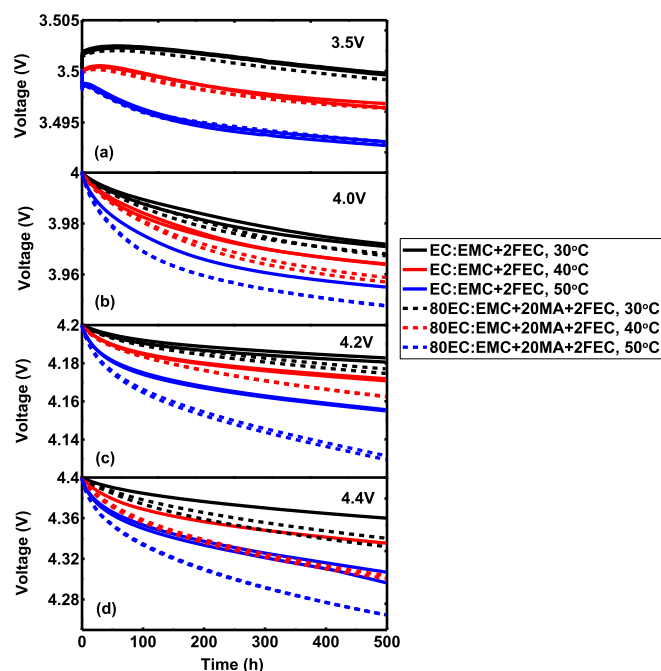
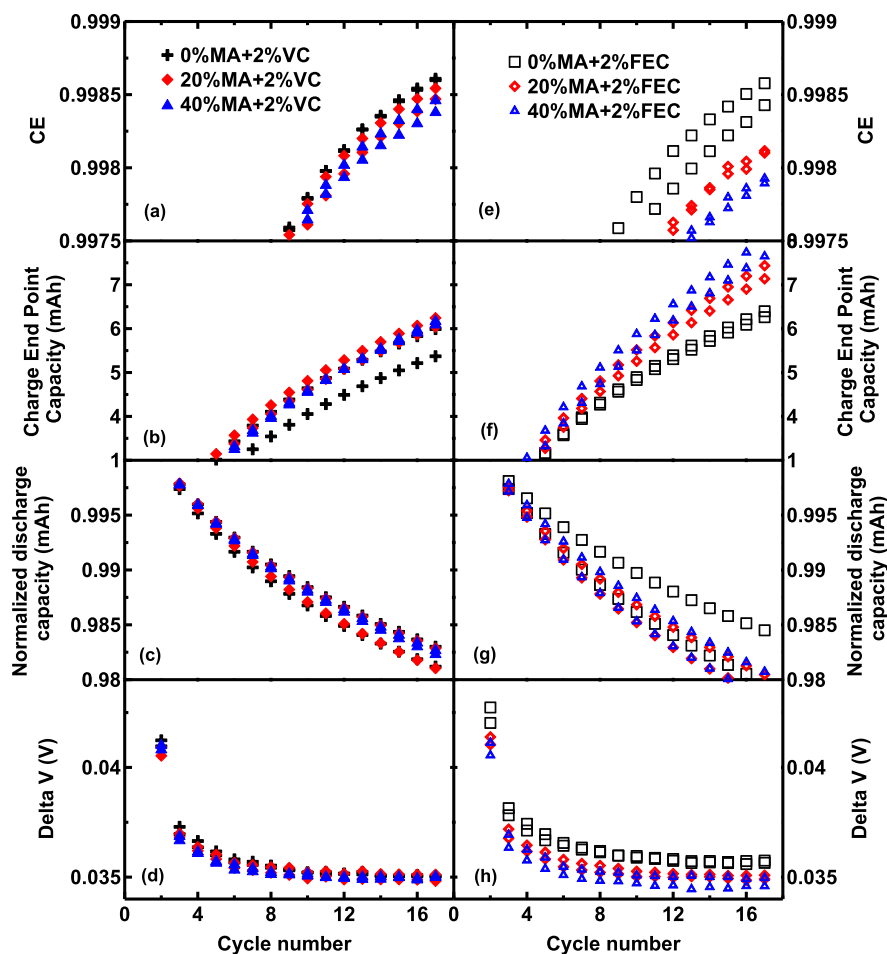


Fig. 7. Open circuit potential versus time of NMC532/graphite pouch cells containing 0% MA or 20% MA in EC:EMC stored at 30, 40 or 50 °C and at starting potentials of 3.5, 4.0, 4.2 or 4.4 V.

lithium plating at 2C. Fig. 4b shows that incorporating 20% and 40% MA as a co-solvent significantly improved the capacity retention of all cells when charged at 2C, either when 2% VC or 2% FEC was used. The cells with EC:EMC:DMC +40% MA + 2% FEC performed the best with no apparent capacity fade even when charged at 2.5C. Fig. 4c shows the impact of 20% and 40% MP on the pouch cells. Similarly, all cells showed no obvious capacity fade when charged at 2C. But all cells containing MP started to undergo unwanted lithium plating at 2.5C. So MP added to the electrolyte did not improve the charging rate capability of cells as much as when MA was added, which is consistent with the lower ionic conductivity of the MP-containing electrolytes compared to the MA-containing electrolytes at 20 °C, as shown in Fig. 1.

The difference between the average charge voltage and the average discharge voltage, ΔV, gives information about the internal impedance of the cell. If ΔV increases with cycle number under the same charge and discharge current it is a sign of serious cell degradation, in the case of these studies, caused by unwanted lithium plating [1,2]. Smaller and stable values of ΔV with cycle number are desired. Fig. 4d, e and f shows ΔV versus cycle number for the cells of Fig. 4a, b and c. By comparing Fig. 4d, e and 4f to Fig. 4a, b and 4c, respectively, it is clear that ΔV begins to increase when unwanted lithium plating begins, as signaled by poor capacity retention.

Fig. 5 shows the UHPC data of cells containing EC:EMC and EC:EMC:DMC, including coulombic efficiency (CE), charge end point capacity, discharge capacity and ΔV, all plotted versus cycle number. A higher CE is generally accompanied by low charge end point capacity slippage and low discharge capacity fade, normally indicating a longer cycling life. Fig. 5a shows that cells containing EC:EMC have higher CE than cells with EC:EMC:DMC regardless of whether 2% VC or 2% FEC are included as additives. Comparing the impact of 2% VC versus 2% FEC, cells with 2%VC show higher CE than cells with 2% FEC for each solvent blend. The changes in the charge end point capacity, the discharge capacity and ΔV of all cells,



**Fig. 8.** UHPC data for NMC532/graphite pouch cells containing up to 40% MA in EC:EMC:DMC solvent with 2% VC (a to d) or 2% FEC (e to h) additives. (a and e): coulombic efficiency; (b and f): charge end point capacity; (c and g): discharge capacity; (d and h):  $\Delta V$ . Data was collected at C/20 between 3.0 and 4.3 V at 40 °C.

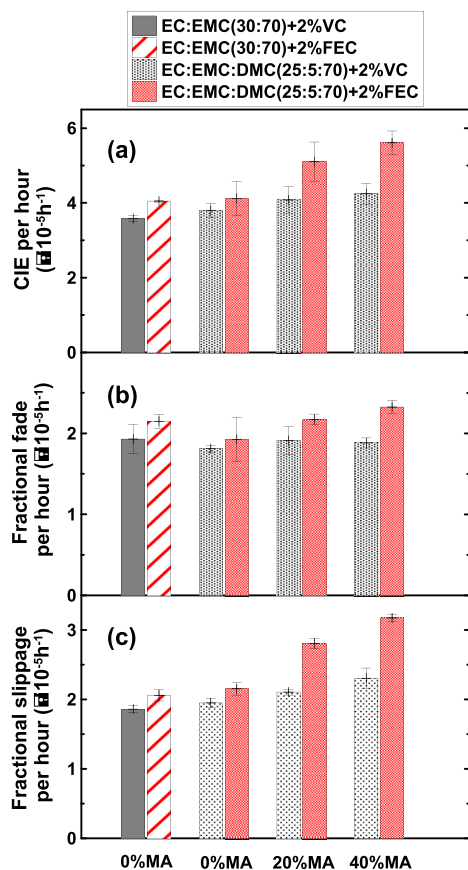
described in Fig. 5b and d respectively, follow trends consistent with the CE trend in Fig. 5a.

Fig. 6 shows the average parasitic heat flow over one cycle between 4.0 V and the indicated upper cutoff potential of cells containing different amounts of EMC, DMC or MA co-solvents and 2% FEC. The experiments were performed sequentially from left to right in Fig. 6. In ester-free solvents, slightly less parasitic heat flow was observed for cells with EC:EMC solvents than for cells with EC:EMC:DMC solvents. The addition of MA caused an increase in parasitic heat flow. The larger the proportion of MA in cells with either EC:EMC or EC:EMC:DMC, the more parasitic heat was produced. Notice that the parasitic heat flow decreased with the increasing upper cut-off voltage from 4.2 V to 4.3 V due to thickening of protective SEI layers with increasing cycle count.

Fig. 7 shows the open circuit voltage of cells containing EC:EMC and 2% FEC during storage experiments at 30 °C–50 °C and at different initial potentials from 3.5 V to 4.4 V. The data in Fig. 7a shows little difference between cells with or without MA. At a full cell potential of 3.5 V, the NMC electrode is on a voltage-charge plateau while the graphite electrode is at a region where the potential varies relatively strongly with state of charge. The fact that the cells with and without MA show the same behaviour during 3.5 V storage suggests electrolyte reduction reactions are not

strongly affected by the addition of MA. Fig. 7b, c and 7d consider the situation when cells are stored nearer to the top of charge where the graphite electrode is on a voltage-charge plateau and the NMC electrode is not. A comparison between the cells containing 0% MA and 20% MA in Fig. 7b–d shows that the addition of MA leads to larger voltage drops consistent with an increase in the oxidation of solution species at the positive electrode in the presence of MA. The difference between cells with and without MA is larger at higher potentials and at higher temperature suggesting MA-containing electrolytes with these additives are less stable at higher potentials and at higher temperatures. The results in Fig. 7b–d are consistent with the higher parasitic heat flows observed in Fig. 6 for cells containing MA.

Fig. 8 shows the UHPC data of cells containing 0%, 20% and 40% MA. Fig. 8a and d shows the results for cells with 2% VC and Fig. 8e and h shows results for cells with 2% FEC. In Fig. 8a and e, the CE of cells with MA was slightly lower than the cells without MA after 16 cycles. Therefore, in agreement with Figs. 6 and 7b–d, adding MA to cells will compromise long term lifetime as a tradeoff for high rate charge capability, at least with the electrolytes and additives used here. Fig. 8 shows that cells with 2% VC outperformed cells with 2% FEC. In Fig. 8b, cells with 20% MA show slightly higher charge end point capacity slippage than cells with 0% MA in the case of 2% VC.



**Fig. 9.** Effect of MA on the coulombic inefficiency per hour (CIE) (a), the fractional fade per hour (b) and the fractional slippage per hour (c) of NMC532/graphite pouch cells. Raw data is shown in Fig. 8 and was collected at C/20 between 3.0 and 4.3 V at 40 °C.

The difference between adding 20% MA and 40% MA was almost negligible in cells with 2% VC, while the negative effect of adding more MA for cells with 2% FEC is much more visible, as shown in Fig. 8f. The normalized discharge capacity versus cycle number of the cells is shown in Fig. 8c and g, corresponding to cells with 2%VC and 2% FEC, respectively. No dramatic differences were observed when different amounts of MA were added. All cells show similar  $\Delta V$  changes in Fig. 8d and h.

Fig. 9 summarizes the coulombic inefficiency (CIE) per hour, fractional fade per hour and fractional charge end point capacity slippage per hours that were calculated from the data measured during cycles 11–16 in Figs. 5 and 8. In Fig. 9a, cells with EC:EMC show lower CIE (better) than cells with EC:EMC:DMC and the CIE increased with higher MA proportions (bad) in cells with EC:EMC:DMC, no matter if the additive was 2% VC or 2% FEC. Fig. 9b and c shows the corresponding fractional fade and fractional slippage, respectively. All cells with 2% VC show very similar fractional fade, indicating that the changes to the CIE that occur with different solvent blends is mainly derived from the changes to the fractional charge endpoint capacity slippage which is consistent with Fig. 7b–d. In other words, these electrolytes with DMC are prone to be oxidized more easily than those with EMC at the positive electrode and the addition of MA further increases the rate of oxidation. This same scenario also applies to cells with 2% FEC, which show the same trend in the fractional charge endpoint capacity slippage.

Due to the large deviation in the fractional fade for some pair cells with EC:EMC:DMC, it is difficult to compare cells with EC:EMC to those with EC:EMC:DMC. However, additions of MA to cells with EC:EMC:DMC did increase the fade. It appears that 2% FEC is not able to protect the electrodes well as 2%VC, leading to increased capacity loss with cycle number.

Fig. 10 shows the long-term cycling data of cells containing 0%, 20% and 40% MA or MP in EC:EMC:DMC at 40 °C, with 2% VC (left panels) or 2% FEC (right panels). Fig. 10a and b shows discharge capacity versus cycle number. Fig. 10c and d shows normalized capacity versus cycle number. Fig. 10e and f shows the corresponding  $\Delta V$  versus cycle number. Clearly, cells show worse capacity retention in the presence of more ester in agreement with expectations based on Figs. 6, 7 and 9. At each proportion of ester, MA is more beneficial to capacity retention than MP, with 2% VC or 2% FEC. A head-to-head comparison between 2% VC and 2% FEC, with or without ester, indicates that 2% VC outperforms 2% FEC, consistent with the UHPC results in Fig. 9. Fig. 10e shows that 20% and 40% esters slightly increase the rate of impedance growth for cells with 2%VC, while 20% and particularly 40% ester in cells with 2% FEC led to more significant rates of impedance growth (see Fig. 10f).

#### 4. Conclusions

In the  $\text{Li}[\text{Ni}_{0.5}\text{Mn}_{0.3}\text{Co}_{0.2}]\text{O}_2/\text{graphite}$  pouch cells studied here, cells with EC:EMC:DMC solvent show better high rate charging performance than cells with EC:EMC, and adding methyl acetate (MA) or methyl propionate (MP) to EC:EMC:DMC further enhanced the high rate charging capability significantly. The fast charging improvement is mainly due to the highly conductive ester co-solvents coupled with suitable additives, and herein 2% FEC outperformed 2% VC as far as fast charge capability is concerned. Cells containing 40%MA and 2% FEC showed the highest fast charge capability of 2.5C.

Unfortunately, the high rate charging capability of ester-containing cells is compromised by a tradeoff in lifetime. The parasitic heat flow increased with the amount of MA co-solvent added to the cells and cells with 2% FEC produced more heat flow than cells with 2% VC. Open circuit voltage versus time of cells stored at 4.0, 4.2 or 4.4 V containing 2% FEC and 0% or 20% MA showed that the esters increase the rates of parasitic reactions with increasing voltage or increasing temperature. The shorter lifetime of cells containing MA was confirmed by UHPC measurements and long-term cycling at 40 °C. The UHPC results also predicted that cells with 2% FEC would have shorter lifetimes than cells with 2% VC.

This work clearly shows that lithium-ion cell manufacturers can improve the fast charge capability of NMC/graphite cells with relatively large electrode loadings ( $3.5\text{--}4.0\text{ mg/cm}^2$  at the positive) and relatively dense electrodes ( $3.5\text{ g/cm}^3$ ) by incorporating modest amounts of methyl acetate in the electrolyte. The authors are aware of several commercially available NMC and NCA Li-ion power cells that do include methyl acetate in their electrolyte. However, the use of esters does cause a lifetime penalty in low rate cycling at elevated temperatures at least with the electrolytes considered in this paper. It is very important to understand the detailed chemistry that occurs in methyl acetate-containing cells which limits lifetime and that is a strong focus of our future work. It may also be the case that more sophisticated electrolytes and electrolyte additive sets can be found that eliminate this lifetime penalty (without impacting the fast charge capability) and that will

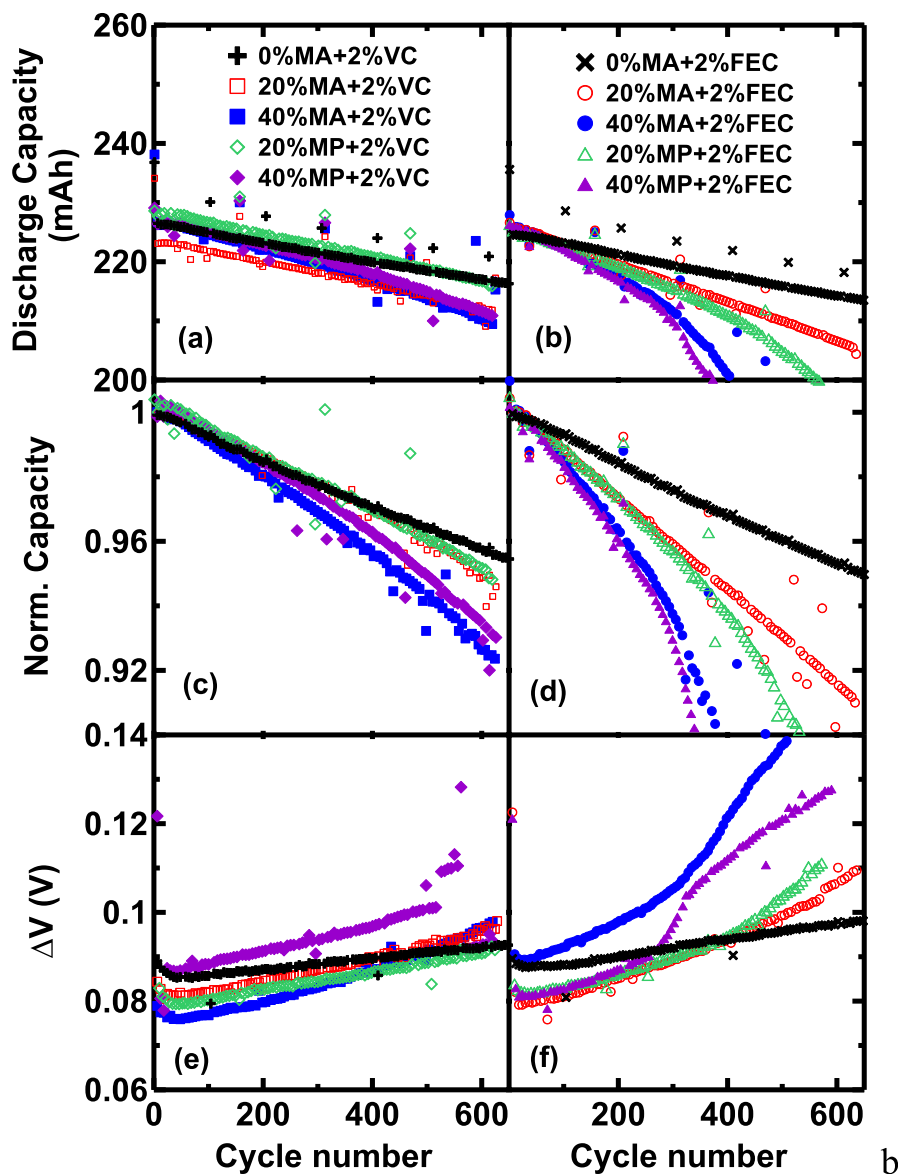


**Fig. 10.** Capacity (3.0–4.3 V, C/3 CCCV and  $40 \pm 0.1$  °C) and corresponding  $\Delta V$  versus cycle number of NMC532/AG pouch cells with EC:EMC:DMC as the base solvent. (a): discharge capacity versus cycle number of cells containing MA or MP with 2% VC; (b) discharge capacity versus cycle number of cells containing MA or MP with 2% FEC; (c) normalized capacity versus cycle number of cells with 2% VC; (d) normalized capacity versus cycle number of cells with 2% FEC; (e)  $\Delta V$  versus cycle number of cells with 2% VC; (f)  $\Delta V$  versus cycle number of cells with 2% FEC.

be another focus of future work. The benefits of methyl acetate for improving fast charge capability are hard to ignore.

#### Acknowledgements

The authors would like to thank Tesla Canada and the Natural Science and Engineering Research Council of Canada (NSERC) for financial support under the auspices of the Industrial Research Chairs program. The authors thank Dr. Jing Li of BASF for supplying most of the electrolyte solvents and additives used in this work. SLG thanks NSERC and the Walter C. Sumner Foundation for Scholarship support. LM thanks the Killam Trusts for scholarship support.

#### References

- [1] Q.Q. Liu, D.J. Xiong, R. Petibon, C.Y. Du, J.R. Dahn, J. Electrochem. Soc. 163 (2016) A3010.
- [2] Q.Q. Liu, R. Petibon, C.Y. Du, J.R. Dahn, J. Electrochem. Soc. 164 (2017) A1173.
- [3] J.C. Burns, D.A. Stevens, J.R. Dahn, J. Electrochem. Soc. 162 (2015) A959.
- [4] M.C. Smart, B.V. Ratnakumar, K.B. Chin, L.D. Whitcanack, J. Electrochem. Soc. 157 (2010) A1361.
- [5] H.-C. Shiao, D. Chua, Hsiu-ping Lin, S. Slane, M. Salomon, J. Power Sources 87 (2000) 167.
- [6] S.V. Sazhin, M.Y. Khimchenko, Y.N. Trittenichenko, H.S. Lim, J. Power Sources 87 (2000) 112.
- [7] S. Herreyre, O. Huchet, S. Barusseau, F. Perton, J.M. Bodet, Ph Biensan, J. Power Sources 97–98 (2001) 576.
- [8] A. Ohta, H. Koshina, H. Okuno, H. Murai, J. Power Sources 54 (1995) 6.
- [9] M.C. Smart, B.V. Ratnakumar, S. Surampudi, J. Electrochem. Soc. 149 (2002) A361.
- [10] M.C. Smart, B.V. Ratnakumar, S. Surampudi, Y. Wang, X. Zhang,

- S.G. Greenbaum, A. Hightower, C.C. Ahn, B. Fultz, J. Electrochem. Soc. 146 (1999) 3963.
- [11] Shin-Ichi Tobishima, K. Hayashi, Kei-Ichi Saito, Jun-Ichi Yamaki, *Electrochim. Acta* 40 (1995) 537.
- [12] S. Herreyre, P. Biensan, F. Pertion, S. Barusseau, US6399255 B2 (1998).
- [13] R. Petibon, J. Harlow, D.B. Le, J.R. Dahn, *Electrochim. Acta* 154 (2015) 227.
- [14] R. Petibon, C.P. Aiken, L. Ma, D. Xiong, J.R. Dahn, *Electrochim. Acta* 154 (2015) 287.
- [15] X. Ma, R.S. Arumugam, L. Ma, E. Logan, E. Tonita, J. Xia, R. Petibon, S. Kohn, J.R. Dahn, J. Electrochem. Soc. 164 (2017) A3556.
- [16] A.J. Smith, J.C. Burns, S. Trussler, J.R. Dahn, J. Electrochem. Soc. 157 (2010) A196–A202.
- [17] L.E. Downie, K.J. Nelson, R. Petibon, V.L. Chevrier, J.R. Dahn, *ECS Electrochem. Lett.* 2 (2013) A106.
- [18] L.J. Krause, L.D. Jensen, J.R. Dahn, J. Electrochem. Soc. 159 (2012) A937.
- [19] K.L. Gering, *Electrochim. Acta* 51 (2006) 3125.
- [20] K.L. Gering, *ECS Trans.* 1 (2006) 119.
- [21] K.L. Gering, *Electrochim. Acta* 225 (2017) 175.